

NCAT Report 20-04

**INFLUENCE OF ASPHALT
PAVEMENT CHARACTERISTICS
ON VEHICULAR ROLLING
RESISTANCE**

**Fan Gu
Randy West
Buzz Powell**



June 2020



277 Technology Parkway ■ Auburn, AL 36830

Influence of Asphalt Pavement Characteristics on Vehicular Rolling Resistance

NCAT Report 20-04

By

Dr. Fan Gu, P.E.
Assistant Research Professor
National Center for Asphalt Technology

Dr. Randy West, P.E.
Director and Research Professor
National Center for Asphalt Technology

Dr. Buzz Powell, P.E.
Assistant Director
National Center for Asphalt Technology

Sponsored by
National Asphalt Pavement Association

June 2020

ACKNOWLEDGEMENTS

The authors wish to thank the National Asphalt Pavement Association for sponsoring this research project and for providing technical review of this document. The authors also gratefully acknowledge the following members and friends of the NCAT Applications Steering Committee for their review of this technical report: Heather Dylla, Gerry Huber, Cheng Ling, Nathan Morian, Derek Nener-Plante, Nadarajah Sivaneswaran, and Christopher Wagner.

DISCLAIMER

The contents of this report reflect the views of the authors who are responsible for the facts and accuracy of the data presented herein. The contents do not necessarily reflect the official views or policies of the sponsoring agency, the National Center for Asphalt Technology or Auburn University. This report does not constitute a standard, specification or regulation. Comments contained in this paper related to specific testing equipment and materials should not be considered an endorsement of any commercial product or service; no such endorsement is intended or implied.

TABLE OF CONTENTS

1 Introduction	5
2 Research Objective	6
3 Measurement of Rolling Resistance	6
4 Pavement Properties Affecting Rolling Resistance	10
5 Low Rolling Resistance Asphalt Mix Design and Implementation	14
6 Summary and Conclusions	16
References	18

1 INTRODUCTION

Rolling resistance is typically considered to be the longitudinal force resisting a vehicle's tires as they roll across the pavement surface. This concept is limited to steady-state, free-rolling conditions (Aldhufairi and Olatunbosun 2018). A more precise definition of rolling resistance is the mechanical energy loss (e.g., heat dissipation) by a tire rolling for a unit distance of roadway (Schuring 1977). Significant components of rolling resistance include tire hysteresis damping, aerodynamic drag, and tire-pavement interaction. Factors that influence rolling resistance include air temperature, vehicle speed, and tire-inflation pressure. Although many of the factors that affect rolling resistance are environment and vehicle dependent, properties of the pavement also influence the overall rolling resistance of a vehicle. The three pavement properties commonly thought to affect vehicular rolling resistance include pavement roughness (i.e., smoothness), surface texture, and pavement stiffness. The roughness-related energy loss is associated with the working of vehicle suspension components, drivetrain components, and deformation of tire sidewalls. The texture-related energy loss is attributed to the contact between the tire tread and pavement surface within the macrotexture range (e.g., texture wavelengths from 0.5 mm to 50 mm). The stiffness-related energy loss is due to the energy dissipation from pavement deformation.

Several studies have shown that for the surface transportation sector, a 10% reduction in rolling resistance generally results in a 1 to 3% decrease of fuel consumption and a 1 to 4% decrease of greenhouse gas (GHG) emissions (National Research Council 2006, Wang et al. 2012, Riemersma and Mock 2012). According to *Annual Energy Review*, the transportation sector consumed approximately 28% of total energy in the United States in 2018, with on-road vehicles accounting for 78% of the consumption (EIA 2019). If it is possible to reduce rolling resistance of all pavements in the U.S. by 10%, it is estimated that \$12.5 billion could be saved and 36.5 million tons of GHG emissions could be reduced every year.

Because of such potential benefits, several studies have been performed to reduce the rolling resistance of vehicles and pavements, mainly focusing on the optimization of tires and pavement characteristics. For instance, the Environmental Protection Agency pointed out that single wide-base tires and wheels are lighter than standard dual tires and wheels, which results in a potential fuel economy improvement of 2 to 5% (EPA 2016). Aldhufairi et al. (2019) designed a multi-chamber tire with a 40% reduction in rolling resistance while maintaining tire grip and corner-handling. Ejsmont et al. (2017) evaluated the influence of pavement surface texture on rolling resistance. They established a regression model to relate pavement texture, as measured by mean profile depth (MPD), to the coefficient of rolling resistance. Pettinari et al. (2016) developed two innovative stone mastic asphalt (SMA) mixes that reduced rolling resistance by 5 to 8%. Espinoza-Luque et al. (2019) reported that these two mixes also exhibited much higher cracking and rutting resistance than the conventional SMA mix in Denmark. Vieira et al. (2019) found that the transverse grinding of asphalt pavement led to more negative surface texture, which decreased rolling resistance by up to 15%.

For pavement life cycle assessments (LCAs), rolling resistance is an important input element in the use phase of a highway project. Santos et al. (2015) developed a life cycle assessment

model for pavement management in Portugal. In that study, rolling resistance was based only on pavement texture, measured by MPD, which was then used to estimate CO₂ emissions. Later, Trupia et al. (2017) proposed an LCA framework that utilized pavement roughness and texture characteristics to estimate the contribution of rolling resistance to the carbon footprint of pavements. Harvey et al. (2016) developed another pavement LCA framework in which pavement-related rolling resistance was included to estimate excess vehicle fuel consumption and emissions. In that framework, excess vehicle fuel consumption and emissions were calculated via three submodels, namely, a structural response submodel, a pavement roughness submodel, and a surface texture submodel, which are further described in the next sections. Since LCAs could affect policy decisions for pavement type selection in the future, understanding how to optimize the rolling resistance of asphalt pavements is crucial for asphalt industry.

2 RESEARCH OBJECTIVE

The objective of this project is to determine if there is sufficient evidence to move forward with field studies to measure rolling resistance of different asphalt mixtures and pavement types and develop an experimental plan for a project to evaluate the rolling resistance of various types of asphalt pavements.

3 MEASUREMENT OF ROLLING RESISTANCE

The methods of measuring rolling resistance are generally divided into two categories: laboratory and field methods (Sandberg et al. 2011). The laboratory method measures the interaction force between a vehicle tire and a rotating drum, which is usually called the drum method. As shown in Figure 1, a normal force is applied to a tire that is held against a rotating drum. The tire yields a braking effect to the movement of the drum, which can be quantified by the resistive force at the tire spindle, the resistive torque on the drum hub, the electrical driving power for the motor, or the drum deceleration (or coastdown) when the motor is stopped.



Drum at Technical University of Gdansk
(Sandberg et al. 2011)

Drum at RWTH Aachen University
(Bachmann 2011)

Figure 1. Drum Test Facilities for Measurement of Tire Rolling Resistance

Several test standards have been developed to define the equipment and measurement conditions for the drum method, as summarized in Table 1. Standards from the Society of Automotive Engineering (SAE) and the International Organization for Standardization (ISO) both require a drum with a smooth steel surface or covered by sandpaper material with medium to coarse texture. This is a significant limitation for these methods, since those surfaces are not representative of a road surface. To overcome this shortcoming, some drums have been modified to duplicate typical road surfaces with paving materials cast in polyester or epoxy resins (*Sandberg et al. 2011*). However, the surface irregularities induced by material castings sometimes cause dramatic tire vibration, which thereby affects the accuracy of rolling resistance measurements.

Table 1. Existing Drum Test Standards for Measurement of Tire Rolling Resistance (*Sandberg et al. 2011*)

Test Standard	Measurement Method	Rolling Resistance Indicator	Drum Diameter	Drum Surface	Speed
SAE J1269	Force, torque, power	Force	1.7 m (5.6 ft)	Medium-coarse texture	80 km/h (50 mph)
SAE J2452	Force, torque	Energy loss	1.2 m (3.9 ft)	Medium-coarse texture	115-15 km/h (71-9 mph), coastdown
ISO 18164	Force, torque, power, deceleration	Energy loss	≥1.5 m (4.9 ft)	Smooth	80 km/h (50 mph)
ISO 28580	Force, torque, power, deceleration	Energy loss	2.0 m (6.6 ft)	Smooth	80 km/h (50 mph)

Compared to the laboratory method, the field measurement of rolling resistance is much more complicated due to many confounding factors such as wind resistance, pavement gradients, vehicle transmission loss, and engine friction, etc. (*Ejmont et al. 2016*). Andersen et al. (2015) classified field measurement methods into two subcategories: the trailer method and the fuel consumption method.

The trailer method utilizes a trailer device towed by a moving vehicle to measure the rolling resistance force (F_R) or the angle of deviation (θ), which is then used to calculate the coefficient of rolling resistance (CRR) shown in Equation 1.

$$CRR = \frac{F_R}{F_W} = \tan \theta \approx \theta \quad (1)$$

where CRR is the coefficient of rolling resistance, F_R is the rolling resistance force, F_W is the wheel load, and θ is the angle of deviation. The CRR is used to quantify the rolling resistance between tire and pavement. Figure 2 illustrates the measurement principle of force and angle methods. The force method utilizes a force transducer to measure the reaction force at the wheel spindle and the test tire is mounted on a separate suspension from the trailer. In contrast, the angle method measures the angle of deviation between the pivoted vertical arm and the horizontal axle. Several experimental rolling resistance trailers have been built for passenger car tires and truck tires based on these two principles.

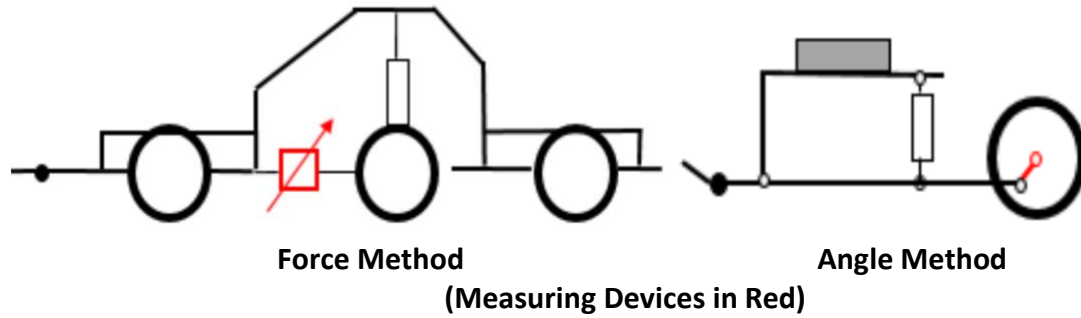


Figure 2. Measurement Principles of Trailer (Anfosso-Ledee et al. 2016)

Figure 3 shows four trailer devices used in recent rolling resistance studies at the French Institute of Science and Technology for Transport, Development and Networks (IFSTTAR) test track and Danish roads, including two Belgian Road Research Center (BRRC) trailers, the Bundesanstalt für Straßenwesen (BASt) trailer, and the Technical University of Gdansk (TUG) trailer. The features of these devices are summarized in Table 2. Note that all of the trailer-based rolling resistance studies have been performed at traffic speeds (e.g., 50-130 km/h or 31-81 mph), which means that these tests do not require lane closures or closed facilities. However, Ejsmont et al. (2012) pointed out that the rolling resistance measurements are not reliable at speeds over 80 km/h (50 mph) if the length of test sections are shorter than 45 meters (148 feet) because the transitions between sections usually yield inaccurate measurements. To ensure accuracy, Anfosso-Ledee et al. (2016) recommended trailer speeds of 80 km/h (50 mph) on highways and arterials, 50 km/h (31 mph) for urban and rural roads, and 30 km/h (19 mph) for inner urban roads. Additionally, test sections should be at least 100 meters (328 feet) long and preferably longer than 500 meters (1640 feet).

Bergiers et al. (2011) conducted a pilot study to compare these devices. They found that the TUG trailer measurements had the lowest variabilities for run-by-run (coefficient of variation [COV] = 1.1%) and day-to-day (COV = 3.8%), whereas the day-to-day COV of the BRRC device and the BASt device was greater than 7%. In addition to these four devices, there are other trailers that have been used less frequently in the field, such as the Forschungsinstitut für Kraftfahrwesen und Fahrzeugmotoren Stuttgart (FKFS) trailer, IPW automotive trailer, Institut für Kraftfahrzeuge (IKA)/ Rheinisch-Westfälische Technische Hochschule (RWTH) Aachen semitrailer, and the Colas trailer. The precision of these trailers for measurement of rolling resistance are still unknown.



BRRC "New" Trailer



TUG Trailer



BRRC "Old" Trailer



BASt Trailer

Figure 3. Trailer-Based Rolling Resistance Measurement Devices (Bergiers 2017)

Table 2. Features of Trailer-Based Equipment to Measure Rolling Resistance

Features	Trailer-Based Equipment			
	BRRC "New"	TUG Trailer	BRRC "Old"	BASt
Method	Force	Angle	Angle	Force
Tire Load	4000 N (899 lbf)	4000 N (899 lbf)	2000 N (450 lbf)	2000 N (450 lbf)
Tire Pressure	200 kPa (29 psi)	210 kPa (30 psi)	200 kPa (29 psi)	200 kPa (29 psi)
Measured Speed	50 km/h (31 mph) 80 km/h (50 mph)	50 km/h (31 mph) 80 km/h (50 mph) 110 km/h (68 mph) 130 km/h (81 mph)	50 km/h (31 mph) 80 km/h (50 mph)	50 km/h (31 mph) 80 km/h (50 mph)
Field Application	IFSTTAR Track (France)	IFSTTAR Track (France) COOEE Section (Denmark) MnROAD (US)	IFSTTAR Track (France)	IFSTTAR Track (France)

Pavement temperature has a significant influence on rolling resistance measurements. The ROSANNE project recommended that rolling resistance tests be conducted at air temperatures between 5°C (41°F) and 35°C (95°F) with a reference temperature of 20°C (68°F) (Anfosso-Ledee *et al.* 2016). If measurements are conducted at air temperatures other than 20°C, a temperature correction shall be made by means of Equation 2.

$$C_{ref} = C_T \left[1 + k(T - T_{ref}) \right] \quad (2)$$

where C_{ref} is the coefficient of rolling resistance at the reference temperature [i.e., 20°C (68°F)], C_T is the coefficient of rolling resistance at the testing temperature, T is the testing temperature, T_{ref} is the reference temperature, and k is the temperature correction factor that varies with the tire type.

Compared to the coefficient of rolling resistance, measurements of fuel consumption are another, less direct indicator of rolling resistance. This is because fuel consumption is influenced by many other factors besides rolling resistance, including pavement grade and curvature, vehicle speed, engine efficiency, and weather. Thus, isolating rolling resistance from the other factors is more challenging for the fuel consumption approach to quantifying rolling resistance.

Heffernan (2006) conducted fuel consumption measurements for heavy trucks at the NCAT Test Track. He eliminated the effect of pavement grade from measured fuel consumption but was unable to establish a reliable relationship between fuel consumption and pavement characteristics (i.e., roughness and texture). He attributed the lack of precision of fuel consumption measurement to sensor noise and the short lengths of each test section.

Chatti and Zaabar (2012) measured the fuel consumption of five different types of vehicles (i.e., medium car, SUV, van, light truck, and articulated truck) at five different locations in Michigan. The sections included both asphalt and concrete pavements with varying from 0.8 to 7.6 km (0.5-4.7 miles) in length, international roughness indexes (IRI) ranging from 0.5-6 m/km (32-380 inch/mile), and mean profile depths (MPD) varying from 0.2-2.0 mm. In addition to these pavement characteristics, they also evaluated vehicle characteristics including engine efficiency and weather conditions. They found that both pavement roughness and surface texture exhibited positive linear relationships with the measured fuel consumption. This demonstrated that if the test section is long enough, the fuel consumption method is capable of assessing the rolling resistance of pavements with different surface characteristics.

Perrotta et al. (2018, 2019) investigated modern truck logistics and telematics databases in the United Kingdom and collected vehicle characteristics, pavement characteristics, weather conditions, and the associated fuel consumption. They utilized two machine learning approaches including random forest and neural network model to estimate the fuel consumption related to the rolling resistance of pavement. They concluded that neural network modelling is a reliable approach to evaluate the impacts of pavement roughness and texture on fuel consumption.

Harvey et al. (2016) designed an experimental plan for the fuel consumption measurement of 23 test sections in California, which included asphalt, concrete and composite pavements with a variety of surface characteristics. All sections were selected to have lengths of at least 1 km (0.6 mile) with no horizontal curves and average slope less than 0.5 percent. This project is still ongoing, and the final report is anticipated to be published in 2020.

4 PAVEMENT PROPERTIES AFFECTING ROLLING RESISTANCE

As previously noted, the three pavement characteristics that affect vehicular rolling resistance are surface texture, roughness, and stiffness. Surface texture results in a loss of energy through

deformation of tire tread rubber in the tire-pavement contact area (Shakiba et al. 2016). Pavement roughness generates deflections and vibrations in the suspension system of vehicle, which are absorbed by the shock absorbers causing a loss of energy. Pavement stiffness affects pavement deflections under traffic loading, which results in energy loss associated with material damping and inelasticity.

Pavement surface texture is defined as the deviations of the pavement surface from a true planar surface (Hall et al. 2009). The Permanent International Association of Road Congress divides pavement surface texture into four levels in terms of the wavelength of the deviation, which include:

- Microtexture with wavelengths from 0 mm to 0.5 mm,
- Macrottexture with wavelengths from 0.5 mm to 50 mm,
- Megattexture with wavelengths from 50 mm to 500 mm, and
- Unevenness with wavelengths from 500 mm to 50 m.

Sandberg and Ejsmont (2002) related these pavement texture levels to the different tire-pavement interaction characteristics, as presented in Figure 4. As illustrated, rolling resistance is dependent on macrottexture, megattexture, and unevenness of pavement surface.

Macrottexture is often quantified by the mean texture depth using circular texture meter (ASTM E2157) or sand patch method (ASTM E965), or MPD using a vehicle-mounted laser device (ASTM E1845). Megattexture and unevenness of pavement surface is represented by the pavement smoothness and quantified by IRI.

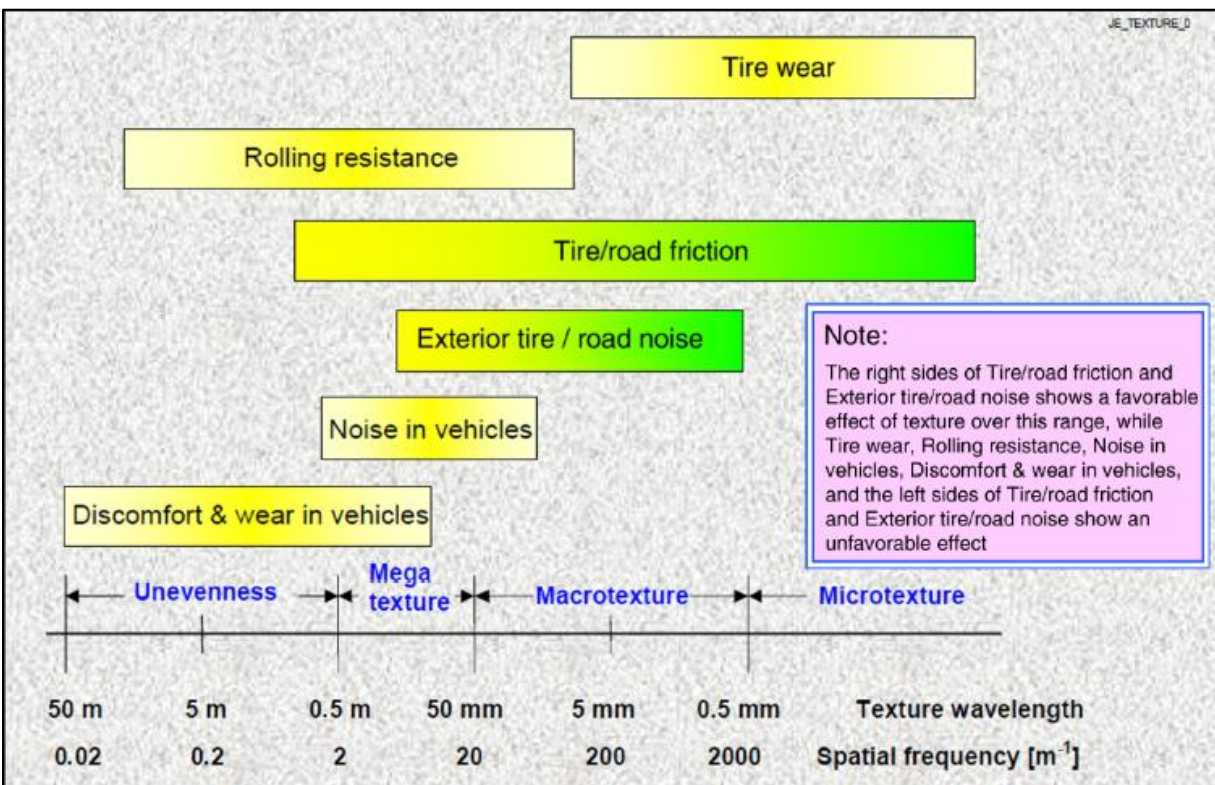


Figure 4. Effects of Pavement Texture Levels on Tire-Pavement Interaction Characteristics (Sandberg and Ejsmont 2002)

Numerous researchers from the European Union have investigated the relationship between CRR and pavement surface characteristics (e.g. MPD and IRI) using multiple linear regression analyses. As shown in Table 3, CRR has a strong linear correlation with MPD and IRI according to rolling resistance measurements from IFSTTAR. However, Ejsmont et al. (2012) conducted a rolling resistance testing at MnROAD test sections, and Sohaney and Rasmussen (2013) found that the existing linear regression models exhibited poor agreement with the measured data from MnROAD. The potential reasons for this are that the temperature correction procedure established in the ROSANNE project might not be applicable to MnROAD sections, and/or the measurements of CRR and MPD might be inaccurate (Ejsmont et al. 2012). Anfosso-Ledee et al. (2016) found another linear relationship between the CRR and the laser-measured macrotexture parameter, level of macrotexture (LMA). However, no other studies were performed to validate this relationship. In general, pavement surface texture is recognized to considerably influence rolling resistance, but there is no agreement on which texture parameter is best correlated with rolling resistance.

Table 3. Summary of Correlations between CRR and Pavement Surface Characteristics

Reference	Regression Model	R-squared value	Data Source
Sandberg et al. (2011)	$CRR = a + b \times MPD + c \times IRI + d \times IRI \times (v - 20)$	Not Reported	10 routes in Ireland
Bergiers et al. (2011)	$CRR = a + b \times MPD$	>0.70	12 sections at IFSTTAR track
Ejsmont et al. (2016)	$CRR = a + b \times MPD$	>0.90	18 sections at IFSTTAR track
Sohaney and Rasmussen (2013)	$CRR = a + b \times MPD + c \times IRI + d \times Road\ Type$	0.35 (overall)	53 sections at MnROAD
Anfosso-Ledee et al. (2016)	$CRR = a + b \times LMA$	>0.60	12 sections at IFSTTAR track

The impact of pavement structural response (i.e., surface deflection) on rolling resistance is difficult to quantify with the trailer-based CRR and the fuel consumption methods. This is because the measurements for both methods are made at traffic speeds, but it is difficult to measure continuous pavement deflections in real-time. Moreover, for trailer-based CRR measurements, the trailer tire pressure range is only 200-210 kPa (29.0-30.5 psi), which generates a negligible deflection on pavement surfaces. Thus, studies that have primarily focused on the impact of pavement deflection on rolling resistance have relied on modeling.

Coleri and Harvey (2017) used a parameter called excess fuel consumption (EFC) to evaluate the impact of pavement deflection. EFC is defined as the fuel consumption beyond what occurs for an ideal pavement with no energy loss due to deflection. They developed a finite element model, referred to as the OSU (Oregon State University) model, to predict the EFC induced by structural response. They found that pavement stiffness affected EFC by only 0.1% to 0.35%, which is much less than that affected by pavement roughness and texture.

In addition to the OSU model, numerous other pavement deflection-induced rolling resistance models have been developed using either analytical equations or numerical techniques. As shown in Table 4, existing structural rolling resistance models are primarily classified into two categories: finite element models and mechanistic-based analytical models. Most of the finite element models use dissipated energy to quantify the structural impact on rolling resistance,

but this approach is relatively complex and time-consuming. Akbarian et al. (2012) developed a pavement-vehicle interaction model (referred to as the MIT model) to estimate the deflection-contributed fuel consumption by converting the deflection basin into an added road grade. They derived an analytical solution to calculate the surface deflection, which simplified the multi-layered pavement structure as a viscoelastic beam on an elastic foundation. Although using the analytical solution accelerated the computation efficiency, the accuracy of the model prediction is still questionable. Similar to the MIT model, Balzarini et al. (2017) developed a deflection-based rolling resistance model referred to as the MSU (Michigan State University) model, which also assumes that the slope of deflection basin is an added grade against the movement of the wheel. Instead of the analytical deflection model, they used a calibrated finite element model to estimate the deflection basin. Shakiba et al. (2016) developed another deflection-induced rolling resistance model referred to as the UIUC (University of Illinois at Urbana-Champaign), which considered the viscoelastic behavior of asphalt materials and the non-uniform three-dimensional tire contact stresses. Bazi et al. (2018) developed a finite element-based rolling resistance model referred to as UNR (University of Nevada Reno) model, considering the influence moving wheel load on pavement surface deflection. Harvey et al. (2016) compared the predicted EFC among the OSU, MIT, and MSU models. They found that EFC predictions from the OSU and MSU models were comparable but were much greater than those predicted by the MIT model. These mechanistic models have not been calibrated or validated yet through any field study. Harvey et al. (2016) is conducting a fuel consumption study for the California test sections to evaluate the accuracy of the mechanistic rolling resistance models.

In contrast to the mechanistic models, Bennett and Greenwood (2001) developed an empirical-analytical model, referred to as the HDM-4 model, to correlate pavement deflection with vehicular fuel consumption. Chatti and Zaabar (2012) calibrated the HDM-4 model using the fuel consumption data from test sections in the United States. Balzarini et al. (2017) utilized the calibrated HDM-4 model to evaluate the impact of deflection-based rolling resistance on vehicle fuel economy and found that the EFC induced by pavement deflection contributed only 0.1% of the total fuel consumption of a vehicle. They confirmed the findings from Coleri and Harvey (2017) that deflection-based rolling resistance had much less of an impact on vehicle fuel economy compared to surface texture- and roughness-related rolling resistance.

Table 4. Summary of Pavement Deflection-Induced Rolling Resistance Models

Model Name	Model Type	Model Method	Model Validation	Key Reference
OSU Model	Finite element	Dissipated energy	No	Coleri and Harvey 2017
MSU Model	Analytical	Dissipated energy	No	Balzarini et al. 2019
MIT Model	Analytical	Geometry Change of Surface	FWD Data	Akbarian et al. 2012
UNR Model	Finite element	Dissipated energy	FWD Data	Bazi et al. 2018
UIUC Model	Finite element	Dissipated energy	No	Shakiba et al. 2016
HDM-4 Model	Empirical-Analytical	Deflection correlation	Yes	Bennett and Greenwood 2001

5 LOW ROLLING RESISTANCE ASPHALT MIX DESIGN AND IMPLEMENTATION

In 2012, the Danish Road Directorate initiated the project *CO₂ Emission Reduction by Exploitation of Rolling Resistance Modelling of Pavements* (abbreviated as COOEE), to develop a new type of long-lasting asphalt pavement with low rolling resistance, low noise emission, and sufficient friction for traffic safety. To achieve this goal, Pettinari et al. (2016) developed two new stone mastic asphalt (SMA) mixes (denoted as SMA6 COOEE and SMA8 COOEE) with nominal maximum aggregate sizes (NMAS) of 6 mm and 8 mm, respectively. Table 5 presents the particle size distribution of COOEE mixes based on the ISO 565 opening size. Table 6 shows the converted particle size distribution of these mixes according to the ASTM E11 opening size and compares them to the gradation bands for SMA 4.75 and SMA 9.5 mixes. As can be seen, COOEE mixes are finer than the conventional SMA 9.5 mix and coarser than SMA 4.75 mm. According to the feedback from aggregate producers, blending the existing product sizes from their quarries might achieve similar gradation of COOEE mixes. They believed that special fractions would need to be produced for COOEE mixes, and the impacts of the special fractions on other plant products should be evaluated.

Table 5. Particle-Size Distributions for COOEE Mixes – ISO 565 Opening Size

Sieve Size (mm)	SMA8 Ref	SMA8 COOEE	SMA6 COOEE
11.2	100	100	100
8.0	93	95	100
5.6	54	60	96
4.0	38	46	64
2.0	25	32	24
1.0	18	23	18
0.5	14	18	15
0.25	11	14	13
0.125	9	12	12
0.063	8	10	10

Table 6. Particle-Size Distributions for COOEE Mixes – ASTM E11 Opening Size

Sieve Size (mm)	SMA8 Ref	SMA8 COOEE	SMA6 COOEE	SMA 4.75		SMA 9.5	
				Lower	Upper	Lower	Upper
12.5	100	100	100	100	100	100	100
9.5	96	97	100	100	100	70	95
4.75	46	53	79	90	100	30	50
2.36	27	35	31	28	65	20	30
1.18	19	25	19	22	36	-	21
0.6	15	19	16	18	28	-	18
0.3	12	15	13	15	22	-	15
0.075	8	10	10	12	15	8	12

The Marshall mix design method was used to determine asphalt binder type and optimum binder content. As shown in Table 6, a PEN 70/100 asphalt binder was used in the control SMA mix (denoted as SMA8 Ref), and a PMB 40/100-75 asphalt binder was used in the new SMA mixes.

Table 7. Marshall Mix Design for COOEE Mixes

Design Parameter	Mix Type		
	SMA8 Ref	SMA8 COOEE	SMA6 COOEE
NMAS (mm)	8	8	6
Binder Type	PEN 70/100 ¹	PMB 40/100-75 ²	PMB 40/100-75
Binder Content (%)	7.0	7.4	7.9
Air Voids (%)	2.7	2.5	2.4

Note: ¹PEN = Penetration grade; ²PMB = Polymer modified binder

Espinoza-Luque et al. (2019) assessed these binders via the Superpave performance grading system and reported that the PEN 70/100 binder was equivalent to PG 64-28, and PMB 40/100-75 binder was comparable to PG 82-16. They also conducted a series of laboratory performance tests on the SMA mixtures, which included dynamic modulus, Illinois Flexibility Index, and Hamburg wheel track tests. According to NAPA (2002), the SMA specimens were compacted at 6% air voids for performance testing. Figure 3 shows the dynamic modulus master curves of these mixtures at a reference temperature of 21°C (70°F). As presented, both SMA6 COOEE and SMA8 COOEE mixes had higher dynamic moduli at the low frequency domain ($10^{-5} - 10^{-3}$ Hz), and lower dynamic moduli at the high frequency domain (e.g., $10^3 - 10^5$ Hz). Figure 6 demonstrates the results of the Flexibility Index and the Hamburg rut depth. These results also indicate that the COOEE mixes showed higher cracking and rutting resistances than the control mix. In addition, the lab test results easily met the thresholds recommended by Ozer et al. (2016). This demonstrates that both of the designed SMA COOEE mixes could achieve satisfactory long-term performance in the field.

Starting in 2012, the Danish Road Directorate built several test sections in Denmark using the COOEE mixes. Pettinari et al. (2016) comprehensively evaluated the surface texture, friction and rolling resistance of these sections at different times. They found that compared to the SMA8 Ref mix, the SMA6 COOEE and SMA8 COOEE mixes resulted in an average of 5% and 3% reduction of rolling resistance respectively and 15-20% reduction of rolling resistance at a maximum. In addition, the COOEE mixes showed lower surface texture (MPD = 0.64-0.69 mm) but similar friction properties (friction coefficient = 0.54-0.62) as compared to the control SMA mix (MPD = 0.68-0.74mm, friction coefficient = 0.56-0.59), which met Danish requirements for surface mix.

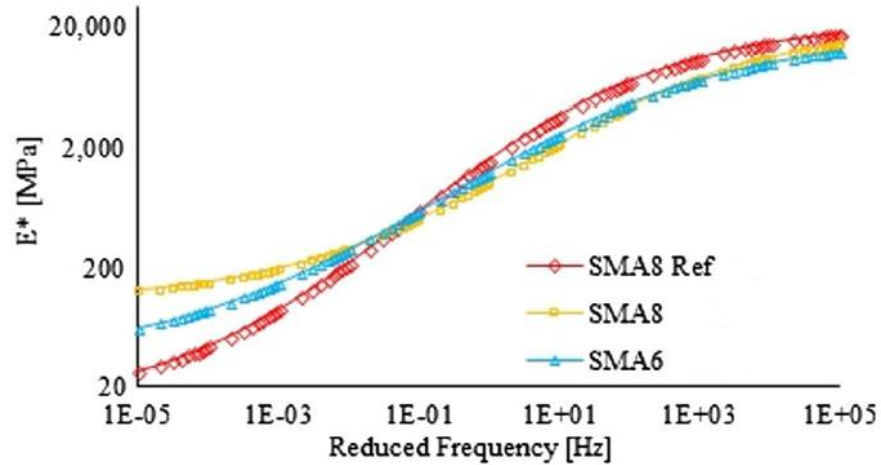


Figure 5. Dynamic Modulus Curves at 21°C Reference Temperature (Espinoza-Luque et al. 2019)

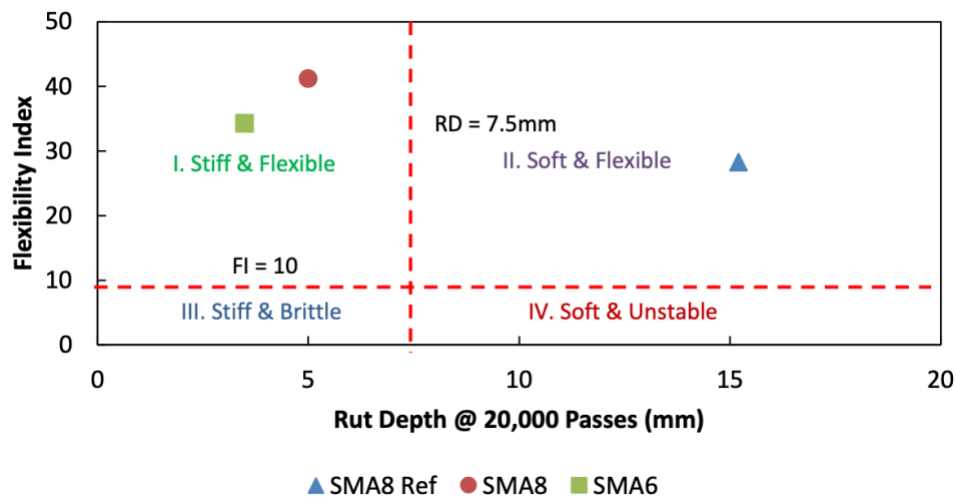


Figure 6. Laboratory Performance Diagram for Low Rolling Resistance Mixes (Espinoza-Luque et al. 2019)

6 SUMMARY AND CONCLUSIONS

Rolling resistance is defined as the energy loss by a tire rolling for a unit distance of roadway. Previous research has indicated that three pavement characteristics mainly affect vehicular rolling resistance: pavement roughness, surface texture, and pavement stiffness. Most studies indicate that pavement roughness and surface texture are more significant than pavement stiffness in terms of the impact on rolling resistance.

Rolling resistance models are not the best way to determine rolling resistance for a pavement. Currently, there are two ways to measure rolling resistance in the field: the trailer method to determine the coefficient of rolling resistance (CRR), and the fuel consumption method to measure rolling resistance-related fuel consumption. For the trailer method, the most repeatable and reliable trailer device is the Technical University of Gdansk (TUG) trailer. Compared to CRR, fuel consumption is a more general indicator of rolling resistance and is

more directly related to vehicle operating cost. The fuel consumption method usually requires much longer test sections than the trailer method.

The Danish Road Directorate optimized the stone mastic asphalt (SMA) mix design to develop a special mix (called COOEE mix) that had low rolling resistance and adequate surface friction. In addition, the COOEE mix showed better cracking and rutting resistances than the control SMA mix in terms of Illinois Flexibility Index and Hamburg wheel tracking tests.

REFERENCES

- Aldhufairi, H., and O. Olatunbosun. Developments in Tyre Design for Lower Rolling Resistance: A State of The Art Review. *Journal of Automobile Engineering*, Vol. 232, No. 14, 2018, pp. 1865—1882.
- Aldhufairi, H., K. Essa, and O. Olatunbosun. Multi-Chamber Tire Concept for Low Rolling-Resistance. *SAE International Journal of Passenger Cars-Mechanical Systems*, Vol. 12, No. 2, 2019, pp. 111—126.
- Akbarian, M., S. Moeini-Ardakani, F. Ulm, and M. Nazzal. Mechanistic Approach to Pavement-Vehicle Interaction and Its Impact on Life-Cycle Assessment. *Transportation Research Record: Journal of the Transportation Research Board*, No. 2306, Transportation Research Board of the National Academies, Washington, D.C., 2012, pp. 171—179.
- Andersen, L., J. Larsen, E. Fraser, B. Schmidt, and J. Dyre. Rolling Resistance Measurement and Model Development. *Journal of Transportation Engineering*, Vol. 14, No. 2, 2015.
- Anfosso-Ledee F., V. Cerezo, R. Karlsson, A. Bergiers, S. Dauvergne, J. Ejsmont, L. Goubert, H. Lesdos, J. Maeck, U. Sandberg, L. Sjogren, and M. Zöller. *Experimental Validation of the Rolling Resistance Measurement Method Including Updated Draft Standard*. ROSANNE Deliverable D3.6, 2016.
- Balzarini, D., I. Zaabar, and K. Chatti. Impact of Concrete Pavement Structural Response on Rolling Resistance and Vehicle Fuel Economy. *Transportation Research Record: Journal of the Transportation Research Board*, No. 2640, Transportation Research Board of the National Academies, Washington, D.C., 2017, pp. 84—94.
- Balzarini, D., K. Chatti, I. Zaabar, A. Butt, and J. Harvey. Mechanistic-Based Parametric Model for Predicting Rolling Resistance of Concrete Pavements. *Transportation Research Record: Journal of the Transportation Research Board*, Vol. 2673, No. 7, Transportation Research Board of the National Academies, Washington, D.C., 2019, pp. 341—350.
- Bazi, G., E. Hajj, A. Ulloa-Calderon, and P. Ullidtz. Finite Element Modelling of the Rolling Resistance due to Pavement Deformation. *International Journal of Pavement Engineering*, 2018, DOI: 10.1080/10298436.2018.1480778.
- Bennett, C., and I. Greenwood. *Modelling Road User and Environmental Effects in HDM-4*. Volume 7: The Highway Development and Management Series, International Study of Highway Development and Management Study, University of Birmingham, U.K. 2001.
- Bergiers, A., L. Goubert, F. Ledee, N. Dujardin, J. Ejsmont, U. Sandberg, and M. Zoller. *Comparison of Rolling Resistance Measuring Equipment—Pilot Study*. MIRIAM SP1 Deliverable No. 3. 2011.
- Bergiers, A. *ROSANNE: Trailer-Based RR Measurement Method*. NAPA/EAPA Asphalt Rolling Resistance Workshop, Brussels, Belgium, 2017.
- Chatti, K., and I. Zaabar. *NCHRP Report 720: Estimating the Effects of Pavement Condition on Vehicle Operating Costs*. Transportation Research Board of the National Academies, Washington, D.C., 2012.
- Chen, D., J. Bilyeu, H. Lin, and M. Murphy. Temperature Correction on Falling Weight Deflectometer Measurements. *Transportation Research Record: Journal of the Transportation Research Board*, No. 1716, Washington, D.C., 2000, pp. 30—39.

- Coleri, E., and J. Harvey. Impact of Pavement Structural Response on Vehicle Fuel Consumption. *Journal of Transportation Engineering, Part B: Pavements*, Vol. 143, No. 1, 2017.
- Ejsmont, J., G. Ronowski, and J. Wilde. *Rolling Resistance Measurements at the MnROAD Facility*. Report No. MN/RC 2012-07, St. Paul, Minn., 2012.
- Ejsmont, J., S. Taryma, G. Ronowski, and B. Swieczko-Zurek. Influence of Load and Inflation Pressure on the Tyre Rolling Resistance. *International Journal of Automotive Technology*, Vol. 17, No. 2, 2016, pp. 237–244.
- Ejsmont, J., G. Ronowski, B. Swieczko-Zurek, and S. Sommer. Road Texture Influence on Tyre Rolling Resistance. *Road Materials and Pavement Design*, Vol. 18, 2017, pp. 181–198.
- Energy Information Administration (EIA). *Annual Energy Outlook 2019 with Projections to 2050*. 2019. Accessed at <https://www.eia.gov/outlooks/aeo/pdf/aeo2019.pdf>.
- Environmental Protection Agency (EPA). *Low Rolling Resistance Tires – A Glance at Clean Freight Strategies*. 2016. Accessed at <https://nepis.epa.gov/Exe/ZyPDF.cgi/P100OW2T.PDF?Dockey=P100OW2T.PDF>.
- Espinoza-Luque, A., I. Al-Qadi, H. Ozer, and M. Pettinari. Laboratory Characterization of Low-Rolling Resistance Danish Stone-Matrix Asphalt. *Journal of Transportation Engineering, Part B: Pavements*, Vol. 145, No. 1, 2019.
- Hall, J., K. Smith, L. Titus-Glover, J. Wambold, Y. Yager, and Z. Rado. *NCHRP Web-Only Document 108: Guide for Pavement Friction*. Transportation Research Board of the National Academies, Washington, D.C., 2009.
- Harvey, J., J. Lea, C. Kim, E. Coleril, Zaabar, A. Louhghalam, K. Chatti, J. Buscheck, and A. Butt. *Simulation of Cumulative Annual Impact of Pavement Structural Response on Vehicle Fuel Economy for California Test Sections*. Report No. UCPRC-RR-2015-05, University of California Pavement Research Center, 2016.
- Harvey, J., J. Meijer, H. Ozer, I. Al-Qadi, A. Saboori, and A. Kendall. *Pavement Life-Cycle Assessment Framework*. Report No. FHWA-HIF-16-014, Washington, D.C., 2016.
- Heffernan, M. *Simulation, Estimation, and Experimentation of Vehicle Longitudinal Dynamics That Affect Fuel Economy*. Masters Thesis, Auburn University, Auburn, Ala., 2006.
- National Asphalt Pavement Association (NAPA). *Designing and Constructing SMA Mixtures: State-of-the-Practice*. Lanham, Md., 2002.
- National Research Council. *Tires and Passenger Vehicle Fuel Economy*. Transportation Research Board Special Report 286, Washington, D.C., 2006.
- Ozer, H., I. Al-Qadi, P. Singhvi, T. Khan, J. Rivera-Perez, and E. El-Khatib. Fracture Characterization of Asphalt Mixtures with High Recycled Content Using Illinois Semicircular Bending Test Method and Flexibility Index. *Transportation Research Record: Journal of the Transportation Research Board*, No. 2575, 2016, pp. 130–137.
- Perrotta, F., T. Parry, L. Neves, and M. Mesgarpour. A Machine Learning Approach for the Estimation of Fuel Consumption Related to Road Pavement Rolling Resistance for Large Fleets of Trucks. *Proceedings of the 6th International Symposium on Life-Cycle Civil Engineering*, Belgium, 2018.
- Perrotta, F., T. Parry, L. Neves, T. Buckland, E. Benbow, and M. Mesgarpour. Verification of the HDM-4 Fuel Consumption Model Using a Big Data Approach: A UK Case Study. *Transportation Research Part D*, Vol. 67, 2019, pp. 109–118.

- Pettinari, M., B. Jensen, and B. Schmidt. Low Rolling Resistance Pavements in Denmark. *Proceedings from the Eurasphalt and Eurobitumen Congress*, Prague, 2016.
- Riemersma, I., and P. Mock. *Influence of Rolling Resistance on CO₂*. International Council on Clean Transportation, Washington D.C., 2012, pp. 1—7.
- Sandberg, U., M. Haider, M. Conter, L. Goubert, A. Bergiers, K. Glaeser, G. Schwalbe, M. Zöller, O. Boujard, U. Hammarström, R. Karlsson, J. Ejsmont, T. Wang, and J. T. Harvey. *Rolling Resistance – Basic Information and State-of-the-art on Measurement Methods*. MIRIAM Final Report, 2011.
- Sandberg, U., and J. Ejsmont. *Tyre/Road Noise Reference Book*. Informex, Sweden, 2002.
- Santos, J., A. Ferreira, and G. Flintsch. A Life Cycle Assessment Model for Pavement Management: Methodology and Computational Framework. *International Journal of Pavement Engineering*, Vol. 16, 2014, pp. 268—286.
- Schuring, D. A new look at the definition of tire rolling loss. *SAE Conference Proceedings of Tire Rolling Losses and Fuel Economy – An R&D Planning Workshop*, Warrendale, Penn., 1977, pp. 31—37.
- Shakiba, M., H. Ozer, M. Ziyadi, and I. Al-Qadi. Mechanics Based Model for Predicting Structure-Induced Rolling Resistance of the Tire-Pavement System. *Mechanics of Time-Dependent Materials*, Vol. 20, 2016, pp. 579—600.
- Sohaney, R., and R. Rasmussen. *Pavement Texture Evaluation and Relationships to Rolling Resistance at MnROAD*. Report No. MN/RC 2013-16, St. Paul, Minn., 2013.
- Trupia, L., T. Parry, L. Neves, and D. Presti. Rolling Resistance Contribution to a Road Pavement Life Cycle Carbon Footprint Analysis. *International Journal of Life Cycle Assessment*, Vol. 22, 2017, pp. 972—985.
- Vieira, T., U. Sandberg, and S. Erlingsson. Negative Texture, Positive for the Environment: Effects of Horizontal Grinding of Asphalt Pavements. *Road Materials and Pavement Design*, 2019.
- Wang, T., I. Lee, A. Kendall, J. Harvey, E. Lee, and C. Kim. Life Cycle Energy Consumption and GHG Emission from Pavement Rehabilitation with Different Rolling Resistance. *Journal of Cleaner Production*, Vol. 33, 2012, pp. 86—96.